

Primljen / Received: 13.3.2019.

Ispravljen / Corrected: 19.10.2019.

Prihvaćen / Accepted: 6.3.2020.

Dostupno online / Available online: 10.4.2020.

## Numerical investigations of interaction between geogrid/wire fabric reinforcement and cohesionless fill in pull-out test

### Authors:



Assist.Prof. **Adis Skejić**, PhD. CE  
University of Sarajevo  
Faculty of Civil Engineering  
[askeja@live.com](mailto:askeja@live.com)  
Corresponding author



Assist.Prof. **Senad Medić**, PhD. CE  
University of Sarajevo  
Faculty of Civil Engineering  
[senad.medic@gf.unsa.ba](mailto:senad.medic@gf.unsa.ba)



Prof. **Tomislav Ivšić**, PhD. CE  
University of Zagreb  
Faculty of Civil Engineering  
[tom@grad.hr](mailto:tom@grad.hr)

Subject review

**Adis Skejić, Senad Medić, Tomislav Ivšić**

### Numerical investigations of interaction between geogrid/wire fabric reinforcement and cohesionless fill in pull-out test

The interaction between geogrid/wire fabric reinforcement and fill material in reinforced earth walls, as well as its quantification, is a complex problem that depends on a number of factors. This paper presents and discusses state of the art related to numerical simulations of pull-out tests used for investigation of interaction between cohesionless fill and reinforcement. In addition, the results of a specially designed group of numerical simulations are presented and compared with recommendations of American and European standards related to such experiments.

**Key words:**

geogrids, geogrid pull-out test, interaction, numerical modelling

Pregledni rad

**Adis Skejić, Senad Medić, Tomislav Ivšić**

### Numerička istraživanja interakcije geomreža/mrežastih armatura i nekoherentnog zasipa u pokusu izvlačenja

Interakcija geomreža/mrežastih armatura i zasipa u zidovima od armiranog tla, kao i njeno kvantificiranje predstavljaju složen problem koji ovisi o brojnim faktorima. U ovom radu su prikazana i komentirana dosadašnja saznanja o numeričkim modelima pokusa izvlačenja kojim se ispituje interakcija armatura i nekoherentnog zasipa. Također su prikazani i rezultati posebno osmišljene skupine numeričkih simulacija, te su uspoređeni s preporukama američkih i europskih normi za provođenje ovakvih pokusa.

**Ključne riječi:**

geomreže, pokus izvlačenja geomreže, interakcija, numeričko modeliranje

Übersichtsarbeit

**Adis Skejić, Senad Medić, Tomislav Ivšić**

### Numerische Untersuchungen zur Wechselwirkung von Geonetzen/Maschenverstärkungen und inkohärenter Verfüllung in einem Expansionsexperiment

Die Wechselwirkung von Geonetzen/Maschenverstärkungen und Verfüllungen in verstärkten Erdwänden sowie deren Quantifizierung stellen ein komplexes Problem dar, die von mehreren Faktoren abhängen. In dieser Abhandlung werden die bisherigen Erkenntnisse über die numerischen Modelle der Expansionsexperimente dargestellt und kommentiert, mit denen die Wechselwirkung von Bewehrungen und inkohärenten Verfüllungen untersucht werden. Darüber hinaus werden auch die Ergebnisse einer speziell entwickelten Gruppe numerischer Simulationen dargestellt und mit den Empfehlungen amerikanischer und europäischer Standards für die Durchführung solcher Experimente verglichen.

**Schlüsselwörter:**

Geonetze, Expansionsexperiment des Geonetzes, Wechselwirkung, numerische Modellierung

## 1. Introduction

Analytical methods based on the principles of rigid body mechanics and limit equilibrium, and extended by empirical coefficients, have been successfully used in the stability analysis of reinforced earth walls since the 1970s [1].

The force transfer mechanism based on these theories is schematically presented in Figure 1: the horizontally placed geogrid supports the active wedge on the one side ("active" zone – action), while it is anchored on the other side into the stable reinforced zone ("passive" zone – resistance). The line that separates these two zones connects the points on the geogrid that correspond to the maximum tensile force in the geogrid, and represents a potential failure surface.

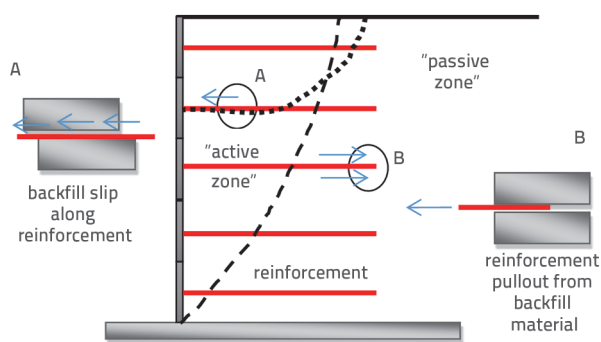


Figure 1. Load transfer in "active" and "passive" zones of reinforced-earth wall

Critical failure mechanisms for checking internal stability of reinforced earth walls are: rupture-tensile failure of geogrid, and pullout of geogrid from the passive anchorage zone [3, 4]. Special pullout tests are conducted to determine the pullout resistance or "anchorage strength" as this resistance is called by some authors [5], and the interpretation is made based on equivalent strength at the backfill and geogrid contact.

The equivalent strength of the contact is the ratio of average shear to normal stress at the geogrid and backfill interface. This strength can *inter alia* be determined by pulling geogrid out of a specially shaped box, and it depends on a great number of factors due to the complexity of interaction between geogrid and backfill. This complex behaviour is further complicated by interaction between the backfill and walls of the box from which the geogrid is pulled.

Numerous authors have used various devices to test the behaviour of geogrid/wire mesh when subjected to pullout action [2, 6-46]. Differences between individual test procedures mainly involve testing equipment, test procedure, and the type and properties of backfill and geogrid [46]. That is why an unambiguous relationship between the limit pullout force and geogrid and backfill properties can not be established based on the results of such different tests. Due to a wide variety of factors that influence the resistance of geogrids to pullout, inconsistencies in the selection of equivalent strength at the contact between geogrid/wire mesh and backfill material have also been registered in numerical

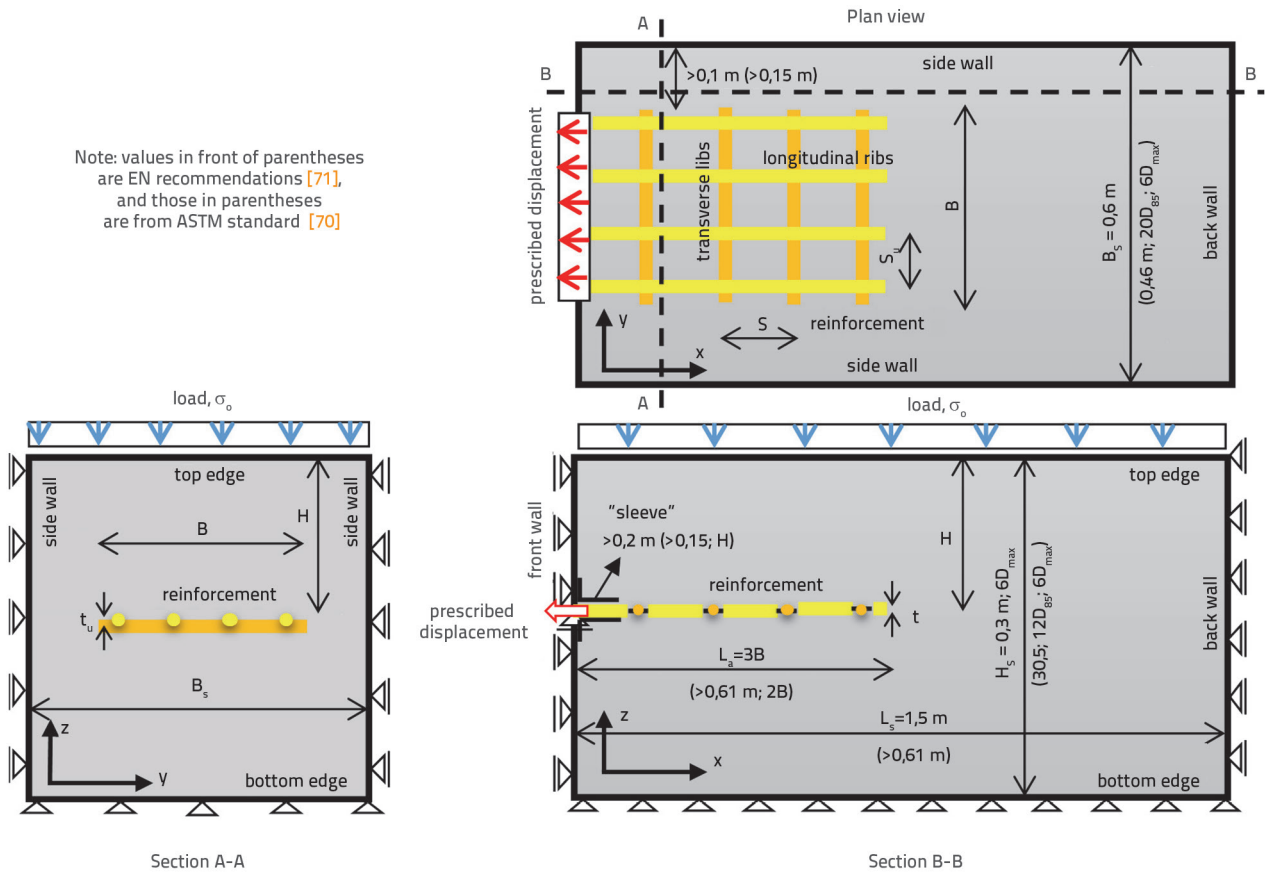
modelling of reinforced earth walls. Thus most researchers accept that the equivalent strength of the contact is equal to the backfill strength [47-60]. This assumption is based on the relatively high pullout resistance of geogrid and wire mesh due to the passive resistance of transverse ribs. In this context, Ling et al. [61] indicate that the conduct of expensive tests aimed at an accurate definition of contact strength at pullout is not at all justified. On the other hand, some authors suggest the use of contact strength - defined via independent pullout test - for modelling backfill and geogrid contacts in walls [31, 62-65]. In these examples, the contact strength is lower than the backfill strength although there are examples in the literature where pullout tests result in (interpreted) contact strength that exceeds the backfill strength [25, 30, 31, 66, 67]. These examples confirm the high complexity of geogrid and backfill interaction mechanisms that are activated during pullout tests.

## 2. Pullout test and equivalent friction coefficient

### 2.1. Pullout test

A specially designed pullout device consists of a box of varying dimensions (length/width/height can vary from 0.25/0.15/0.15 m [68] to 3.4/3.4/1.2 m [69]) in which a geosynthetic or other reinforcing material is placed horizontally, usually at mid-height, and is then pulled out from the front side of the box. Minažek and Mulabdić [35] indicate that more than thirty different pullout devices (differing in size and other properties) have so far been published in the literature. Thus, small, medium-sized, and large-size devices can be differentiated. The same authors indicate that large-size devices, with the box volume ranging from 1 to 2 m<sup>3</sup>, are most frequently used. On average, these devices measure 1.5/0.8/0.7 m (length/width/height). A typical pullout test setup is shown in Figure 2.

Standards providing detailed instructions about the conduct of pullout tests have been developed worldwide. Figure 2 shows recommendations given in the US standard (ASTM D6706) [70] and the European standard (EN 13738) [71] from the aspect of test setup geometry. Recommendations provided in EN standards are given in Figure 2 in the form of dimensions (length measurements) presented in front of parentheses, while the corresponding ASTM measurements are given in parentheses. A sleeve is usually installed at the part of the box from which the geogrid exits. The role of this sleeve is to reduce the influence of the front wall on the pullout resistance value. In some cases, instead of this sleeve, the first transverse rib of the geogrid is installed at a sufficient length from the front edge [66]. There are also examples where expanded polystyrene is installed on the entire surface of the front wall to reduce the influence of its stiffness on the mobilisation of resistance during pullout [28]. The surface of backfill zone in the box can also be subjected to additional load to simulate "in situ" stress (load,  $\sigma_v$ ). The force and displacement are measured during the test at the position of the pullout. The equivalent strength at the geogrid and backfill interface is measured based on the limit force measurements.



Note: values in front of parentheses are EN recommendations [71], and those in parentheses are from ASTM standard [70]

Figure 2. Configuration of the pullout test device: plan view and typical cross-sections with basic elements and indications

Laboratory tests involving pullout of geogrid and wire mesh from the box backfilled with granular material were first conducted in the late 1970s [72-74]. However, significant improvement in the study of interactions at pullout conditions were made by Dyer [75] and Palmeira [66]. They systematically developed a study program and presented pullout test results that pointed to basic mechanisms of the transfer of force from wire mesh to backfill material. It was already known that, in case of geogrids and wire mesh, the pullout resistance is composed of two basic components:

- The friction resistance along longitudinal and transverse ribs,
- The passive resistance of backfill in front of transverse ribs.

The contribution of friction of the soil particles interlocked in wire mesh openings should also be added to these components [35, 76]. The mobilisation of resistance components does not occur simultaneously but, rather, it depends on the magnitude of relative displacement [76, 77]. In case of small relative displacement between the backfill and geogrid, the total friction is mobilised at the contact, while with the further increase of relative displacement the passive resistance of soil is progressively mobilised in front of transverse ribs of the geogrid.

## 2.2. Interpretation of pullout test results

The pullout force, mobilised at limit slip between geogrid and

backfill, is significant for determining equivalent strength at the geogrid and backfill contact. The shear strength at the contact between cohesionless material and geogrid can be defined in several ways, two of which are singled out below:

- Via the equivalent friction coefficient ( $f^*$ ) proposed by Jewell et al. [78]. This coefficient is the ratio of shear stress ( $\tau_{ult}$ ) mobilised at the moment of a full slip of geogrid to the corresponding normal stress at the geogrid and backfill interface ( $\sigma_n$ ), according to the following expression:

$$f^* = \frac{\tau_{ult}}{\sigma_n} = \frac{F_p}{2A\sigma_n} = \frac{F_p}{2L_a B \sigma_n} \tag{1}$$

- where  $F_p$  is the limit pullout force determined during the test,  $L_a$  is the geogrid length, and  $B$  is the geogrid width in accordance with the data given in Figure 2.
- Relatively to the backfill material strength ( $C_i$ ). This value is the ratio of the equivalent coefficient of friction at the interface ( $f^* = \tan \delta$ ) to the friction coefficient of the backfill material ( $\tan \phi$ ), according to the following expression:

$$C_i = \frac{\tan \delta}{\tan \phi} \tag{2}$$

In literature, this ratio is called the interaction coefficient.

### 3. Numerical modelling of pullout test

The definition of the stress-strain state within the pullout box during the testing is significant for three practical aspects:

- to extrapolate results, through simulation of interaction at the pullout test scale, onto the walls and for other test cases that were not investigated by physical modelling due to the great number of combinations of geogrids, backfill materials, and pullout device dimensions,
- to numerically determine geogrid to backfill interaction mechanisms that were not measured or registered by physical modelling due to complexity of such measurements,
- to enable determination of test improvement possibilities by establishing a numerical pullout test model. In other words, numerical simulations can be used to analyse the influence of testing conditions on pullout test results.

Due to significance and great possibilities offered by advanced numerical simulations, it is not surprising that a considerable number of such analyses have so far been published. Numerous studies in which pullout test modelling by complex numerical analyses is proposed, are in most cases conducted using the finite element method and the finite difference method in form of 2D simulations [21, 32, 37, 40, 64, 77, 79-85]. Principal details given in some of these studies are commented on in the following section.

#### 3.1. Overview of published research

An overview of basic characteristics of numerical models (finite element method and finite difference method), starting from the first research conducted by Yogarajah and Yeo [79] to the present day, is given in Table 1.

**Boundary conditions.** Most published analyses are 2D simulations with similar boundary conditions that imply:

**Table 1. Overview of basic properties of published numerical simulations of pullout tests using finite element method and finite difference method**

Author (year), reference	Program	Analysis	Backfill	Geogrid/wire mesh	Backfill and geogrid/wire mesh interface	Front wall
Yogarajah & Yeo (1994), [79]	Sage Crisp	2D, MKE	ME (MC)	LE truss element	MC, zero-thickness elements	Abs. stiff
Shuwang & dr. (1998), [86]	-	3D, MKE	ME (MC)	NLE plate with openings	Nonlinear springs, link elements of the interface	Abs. stiff
Bergado & dr. (2003), [64]	Sage Crisp	2D, MKE	2DE (MC)	LE truss element	MC, zero thickness interface elements	Abs. stiff
Perkins & Edens (2003), [22]	ABAQUS	3D, MKE	SE (BSP)	EPC membrane element	MC, zero thickness interface elements	Abs. stiff
Sugimoto & Alagiyawanna (2003), [77]	-	2D, MKE	2DE (DP)	LE truss element	MC, zero thickness elements	Abs. stiff
Teerawattanasuk & dr. (2003), [87]	FLAC	3D, MKR	SE (MC)	LE solid element	MC, zero thickness elements	Abs. stiff
Palmeira & Dias (2008), [88]	Plaxis	2D, MKE	2DE (MC & HS)	LE „geogrid“ element longitudinal ribs and LE plate element for transverse ribs	MC, zero thickness interface elements	Abs. stiff and smooth
Khedkar & Mandal (2009), [28]	Plaxis	2D, MKE	2DE (MC)	LE „geogrid“ element for longitudinal ribs and LE plate element for transverse ribs	MC, zero thickness interface elements	0.8 cm exp. polystyrene
Alam & dr. (2014), [40]	FLAC	2D, MKR	2DE (MC)	LE 2D element	MC, zero thickness interface elements	Abs. stiff
Rouse & dr. (2014), [89]	FLAC	2D, MKR	2DE (MC)	EP beam element	MC, zero thickness interface elements	Abs. stiff
Abdi & Zandieh (2014) [37]	Plaxis	2D, MKE	2DE (MC)	LE „geogrid“ element for longitudinal ribs and LE plate element for transverse ribs	MC, zero thickness interface elements	1.0 cm exp. polystyrene
Mosallanezhad & dr. (2016), [90]	ABAQUS	3D, MKE	SE (MC)	solid element	MC, zero thickness interface elements	Abs. stiff

*Note:* LE – linear elastic; NLE – nonlinear elastic; EP – elastoplastic; FEM – finite element method; FDM – finite difference method; MC – Mohr Coulomb model, EPC – elastoplastic creep; HS – strain hardening model; BSP – Bounding Surface Plasticity model [91], DP – Drucker Prager model; 2DE – 2D element; SE – solid element

- ideally smooth, horizontally fixed front wall
- horizontally and vertically fixed bottom wall
- horizontally fixed, ideally smooth back wall
- uniformly distributed load on top surface
- controlled force or prescribed displacement at the front end of the geogrid.

As most studies are based on 2D models, side walls of the box-shaped pullout device are ideally smooth, and the model is 1.0 meter in width (plane strain condition).

### Modelling of backfill material

In most published numerical studies, sandy soil is used as backfill material from which geogrid is pulled out. The elastic ideally plastic model (Mohr-Coulomb model) of material behaviour is used in most published numerical simulations. It is known that dense granular material exhibits "softening" behaviour at large shear strains in stress-strain relationships, which is manifested in the reduction of the angle of internal friction and dilation angle (as presented for instance in [92]). Although this behaviour can greatly influence numerical simulation results, the authors are not aware of any published study in which the pullout test would be simulated through such behaviour of backfill material. Besides, examples of constitutive backfill models that include the dependence of the angle of internal friction on normal stress are quite rare. One such investigation was conducted by Rouse and Fannin [89], who demonstrated that it is important to model reduction of the internal friction angle with an increase in normal stress during simulation of tests at vertical stress of less than 50,0 kPa.

### Modelling of geogrid/wire mesh

The most significant difference in published numerical simulations of pullout tests is related to the way geogrid/wire mesh is modelled. That is why published pullout test simulations will be described in this text via four modelling methods. More specifically, details will be presented for the following four pullout test models:

- wire mesh/geogrid is modelled by a thin equivalent cable element – "geogrid" element (line element of unit width).
- wire mesh/geogrid is modelled by longitudinal ribs ("geogrid" element) and transverse ribs (beam element).
- wire mesh/geogrid is modelled by transverse ribs only (stiff 2D element)
- wire mesh/geogrid 3D model (volume elements)

A special interface element is additionally used in all mentioned models at the backfill material and geogrid contact, in order to cover relative displacements (discontinuity in the displacement zone) between the backfill material and geogrid, i.e. the value of slip during pullout. This contact is most often modelled using zero thickness elements with elastoplastic properties (stiffness and strength).

### 3.1.1. Wire mesh/geogrid modelled by equivalent cable element – "geogrid" element

Most published numerical simulations imply pullout of geogrids that is simulated by a line element ("geogrid" element) capable to transfer tensile stress, but they do not include the direct contribution to the resistance as provided by longitudinal and transverse elements of the grid. Yogarajah and Yeo [79] were among the first to propose the idea of numerical modelling of pullout test (Figure 3). They modelled geogrid by a linearly elastic thin cable element of unit width ("geogrid" element), while they simplified the complex behaviour of the geogrid and backfill contact by an interface element of zero thickness [93] with Mohr-Coulomb's constitutive model. Similar models were also used more recently [77, 87]. The primary objective of this pullout test modelling procedure was to numerically confirm the limit value of pullout force by back analysis [64, 77, 79].

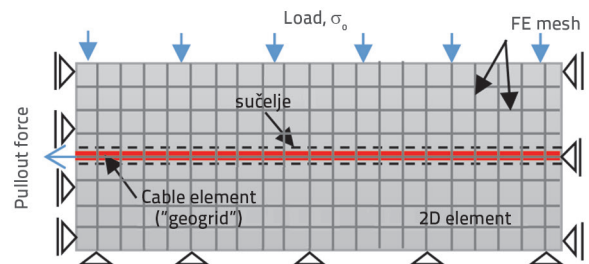


Figure 3. Numerical model of pullout test with wire mesh simulated by cable element of unit width (adopted and modified from [79])

In addition to the mentioned ones, there are other examples of numerical simulations of this type that were aimed at verifying how modelling results are influenced by deformation (rheological) properties of geogrid and contact model [22]. These simulations have revealed that results are not considerably influenced by modelling creep deformation of geogrid, while it has been established that geogrid stiffness and contact properties significantly influence mobilisation of shear stress at the geogrid and backfill material interface.

### Box dimensions

Modeling geogrid by cable element of unit width, and the Mohr-Coulomb model for backfill material, Palmeira and Dias [88] investigated the influence of box top wall stiffness and total box height on the mobilised pullout resistance. These authors investigated the influence of box dimensions on a total of nine models with three box lengths (0,5, 1,0, and 2.0 m), and three box heights (0.3, 0.6, and 1.0). In these simulations, geogrid was placed at mid-height. On the basis of calculated mobilisation resistances it was established that the mobilised pullout resistance reduces with an increase in height. This reduction amounts to approximately 10% for an increase in height ( $H_s$ ) from 0.3 m to 1.0 m, where the increase in height from 0.3 m to 0.6 m does not practically affect the magnitude of the ultimate

pullout force. These results were not interpreted but rather it was established by reference to test results shown in the literature [7, 17] that the box height should be greater than 0.6 m. Numerical simulation results [88] are also related to the influence of sleeve length on the mobilised limit resistance. It was established that an increase in sleeve length causes an increase in limit resistance for the geogrid length of 0.5 m with tensile stiffness of  $EA = 200.0 \text{ kN/m}$ , for the box 1.0 m in height and 1.2 m in length. It should be noted that it was assumed in the analysis that the friction at box walls is reduced by greasing and that it amounts to  $\delta_p = 6^\circ$ . These analyses were conducted with geogrid that was simulated as cable element of unit width, while the sleeve length was simulated by isolating geogrid from the backfill at one part of the sleeve. This is the only example of numerical modelling of a test in which friction at box walls was considered. Although the use of geogrid models simulated by linear cable element ("geogrid" element) has recently been replaced by geogrid models that also include transverse ribs, numerical pullout-test analyses of this type have remained in use to this day [85].

### 3.1.2. Wire mesh/geogrid modelled by longitudinal and transverse ribs

By reviewing the available literature, it was established that 2D reinforcement models with longitudinal ("geogrid" elements) and transverse ribs (plate elements or stiff membrane elements) were used in only four published numerical simulation studies for pullout tests [28, 37, 57, 88].

Palmeira and Dias [88] proposed numerical modelling of reinforcement aimed at comparing numerically predicted and measured results. The comparison was presented in the form of diagrams showing the dependence of displacement and force at the front end of reinforcement, and the magnitude of horizontal pressure at the front wall of the pullout box. The authors consider that the software used offers results that are compatible with measurement results. Nevertheless, this model greatly differs from other mentioned models in one detail. In fact, according to [88] the strength at the contact between longitudinal ribs and backfill material is defined with the interaction coefficient ( $C_1 = 0.95$ ), which means that the backfill and longitudinal ribs friction is practically equal to the backfill material friction. In other papers [28, 37, 57], this friction is modelled with the interaction coefficient  $C_1 < 0.2$ , or the friction of longitudinal ribs is completely neglected [40]. These values of coefficient of interaction between backfill and longitudinal ribs are determined by back analysis based on results obtained by pullout test for isolated longitudinal ribs. As expected, relatively low values of equivalent strength of contact, compared to backfill strength, were obtained because the contribution of longitudinal ribs in the resistance to pullout is much smaller than the contribution of transverse ribs, which is directly covered by the model.

Using the finite element method on a two-dimensional model (Plaxis 2D – [94]), Khedkar and Mandal [28] simulated transverse ribs of specially shaped cellular type steel meshes formed of different-height steel sheets of constant thickness. The numerical model with

its basic elements is shown in Figure 4. Various steel sheet heights were modelled linearly by elastic beam elements that are capable of transferring bending, tension, and compression forces. By varying the spacing of transverse ribs they succeeded in optimising the relationship between the height and distance of steel sheets of the mesh installed in sand. More specifically, the maximum resistance to pullout was realized for the distance to the height ratio of transverse elements of the mesh ( $S/t$ ) amounting to approximately 3.5. After successful verification, the numerical model with reinforcement modelled with longitudinal and transverse ribs was used to estimate the influence of some boundary test conditions on the resistance mobilised at pullout [28].

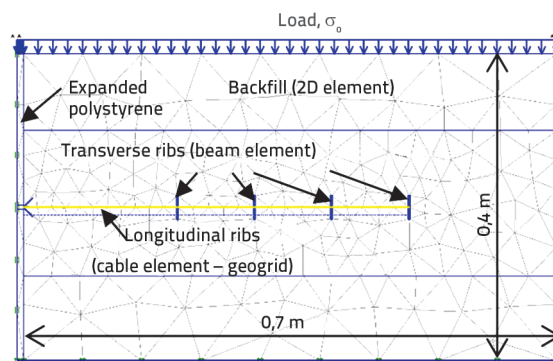


Figure 4. Numerical model of pullout test with reinforcement consisting of longitudinal and transverse ribs, Plaxis 2D [94]: finite element method [28]

The boundary condition assessment methodology involved doubling both dimensions of the box while keeping the reinforcement and transverse rib dimensions constant. When interpreting the plot of total backfill displacement in the box at limit pullout force, the authors concluded that the box dimensions used in the test were adequately selected. In fact, the displacements calculated on the scaled model, at the distance from the front wall equal to the real box length, are negligible. In addition to comparison of the size of the zone affected by displacements, the plot of average effective stress in the box subjected to limit load was also compared. Negligible differences in the magnitude of an average effective stress at box boundary show that further increase in box size, as related to dimensions of the physical model used in the laboratory, would not influence test results.

Abdi and Zandieh [37] used the same numerical model and simulated published measurement results quite successfully. The same authors used numerical simulations to study the influence of box length on the distribution of average effective stress and on the size of the box zone affected by displacements at limit pullout force. The study showed that, for sandy material, the box zone affected by additional average effective stress due to prescribed reinforcement pullout does not cover the area that is more than 20.0 cm away from the free (last) end of reinforcement. According to these results, the authors concluded that the box length of 100.0 cm is adequate for reinforcement 80.0 cm in length.

In both of the above-mentioned studies, the contact between the backfill and transverse ribs is defined by the same strength and

stiffness as for the backfill. Although special sensitivity analyses that would confirm validity of this assumption were not made, it is expected that the strength and stiffness at the interface between transverse ribs and backfill are not of great significance for mobilisation and limit resistance at pullout. In fact, separation of the back part of the transverse rib is enabled by the backfill material model that does not include tensile stress (tension cut-off), while the front side of the transverse rib is driven horizontally into the backfill during realization of the test.

The numerical pullout-test model with the reinforcement simulated in this way could be used for studying the influence of the box and reinforcement geometry and backfill properties on the limit resistance to pullout. Due to the direct contribution of transverse ribs, it is assumed that the influence of backfill and front wall friction, and the influence of backfill height above reinforcement level, could differ from the one determined with reinforcement modelled by cable element of unit width. Such research has been conducted in this paper, as described in detail in Section 4.

### 3.1.3. Wire mesh/geogrid modelled with transverse ribs only

Alam et al. [40] used the finite difference method on the 2D model (FLAC 2D – *Itasca Consulting Group*, 2002 – [95]) to simulate pullout test for a set of transverse ribs under the assumption that the majority of resistance at pullout of inextensible reinforcement is the result of passive resistance of backfill in front of transverse ribs (Figure 5).

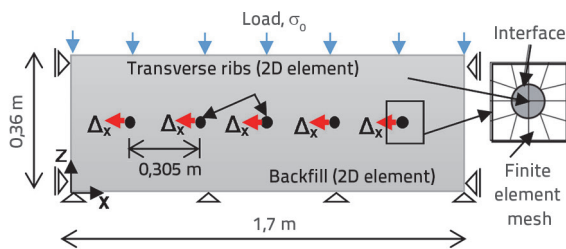


Figure 5. Numerical model of pullout test with reinforcement consisting of transverse ribs only, FLAC 2D: finite difference method (adopted and modified from [40])

Such an approach to numerical modelling with transverse ribs implies only horizontal displacement that can deviate from experimentally measured displacements in the pullout box. This deviation occurs due to the non-symmetrical deformation of transverse ribs as a consequence of volume deformations at the interface. This displacement trend was confirmed by experimental studies [33], which can be simulated by the reinforcement model in the scope of which load is applied at the front end of reinforcement.

### 3.1.4 Three-dimensional wire mesh/geogrid

Palmeira and Dias [88] emphasized that modelling three-dimensional geometry of geogrid/wire mesh could be highly complex, although examples of such modelling do exist. In this

respect, numerical 3D modelling of the pullout test, based on the finite element method with explicit 3D grid geometry, was conducted by Hussein and Meguid [96]. They used the program package ABAQUS 3D (*Dassault Systems Simulia Corp* – [97]) to investigate the influence of individual model parameters on simulation results, and they demonstrated that transverse ribs of the analysed uniaxial geogrid contribute to the resistance to pullout by only 36% of the total resistance. The published numerical simulation does not contain a detailed sensitivity analysis, which confirms that the results do not depend on the finite element mesh density, although this problem can be significant because the geometry of geogrid whose transverse ribs exhibit a very small diameter (about 1.0 mm) was explicitly modelled.

In addition to the above mentioned 3D numerical simulation by the finite element method, results of complex numerical simulations based on the discrete element method have also been published [98]. Furthermore, Tran et al. [99] presented a numerical model that also describes the bending of grid transverse elements at pullout (Figure 6). In this paper, the authors developed a 3D numerical model in which finite elements (FE) and discrete elements (DE) are combined with interface elements that connect FE and DE domains. More specifically, geogrid was modelled with volumetric finite elements (solid elements) and soil with discrete elements.

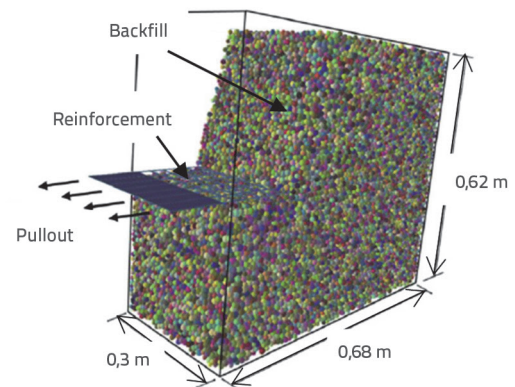
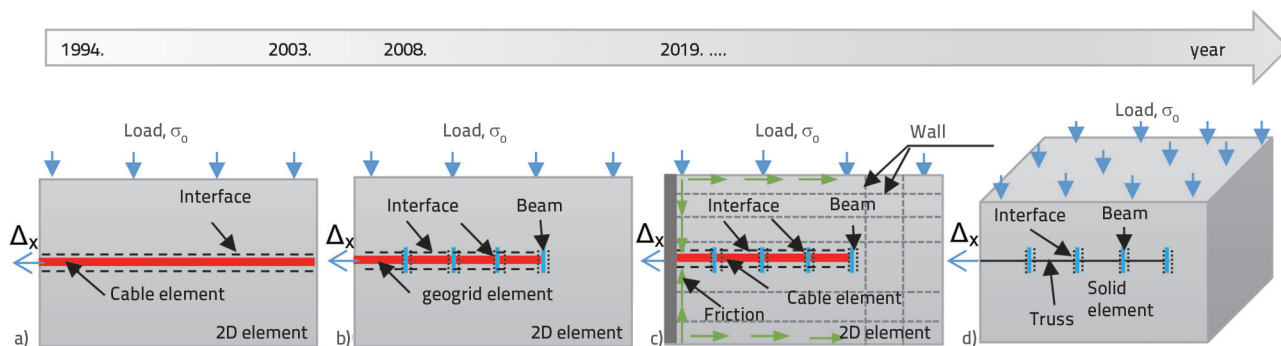


Figure 6. Numerical 3D model representing a combination of finite elements (FE) and discrete elements (DE) [99]

The authors confirmed with this model the measured trend of stress concentration at the front end of extensible geogrids, and they also showed that the implemented model successfully describes the behaviour of extensible grids in pullout conditions. Similar conclusions were made in [100]. In 2016, Bathurst and Ezzein [101] also pointed to limitations regarding practical application of such complex models, namely because numerical simulations of such complexity have not been successfully applied for numerical simulation of structures (walls) made of reinforced earth. Still, some conclusions and ideas arising from the study of geogrid and backfill material interaction based on DEM analysis are presented below.

DEM analysis is appropriate for studying the influence of grain size and geogrid opening on the resistance at the pullout. One such set of simulations was conducted



**Figure 7. Illustration of wire mesh and geogrid models published from 1994 to the present day: a) cable element of unit width with interface element; b) longitudinal ribs (cable element) with interface element and transverse ribs as beam element; c) only transverse ribs and solid 2D element; d) 3D model with explicit geogrid geometry [93]**

by McDowel et al. [102] who demonstrated that the 1:4 ratio of geogrid opening to grain diameter of backfill material is optimal, i.e. that it results in the highest limit resistance at pullout compared to other analysed geometrical configurations (all grains are 40.0 mm in diameter). According to this research, the mentioned ratio of geogrid opening to grain diameter provides for the best interlocking of grains in geogrid openings. A similar study was conducted by Wang et al. [103] who investigated via DEM numerical simulations the influence of the number of transverse ribs on the resistance at the pullout. These authors demonstrated that the limit pullout force increases with an increase in the number of transverse ribs.

There are also examples of studies conducted to determine the influence of backfill compaction, grain shape, and geogrid stiffness, on the backfill to geogrid interaction, but the scope of these studies is mostly limited to successful model verification and to the visualisation of load transfer from geogrid to backfill (e.g. [104, 105]).

The chronology of development of numerical pullout test models based on finite elements and finite difference methods is presented in conclusion of the overview of research conducted so far in this area. Models described in sections 3.1.1 and 3.1.2 are shown in Figures 7.a and 7.b, while models to be used in this paper are presented in figures 7c and 7d (box cross section for 2D models and complete box geometry for 3d model).

Numerical simulations of geogrid tests with the geogrid model that includes openings (apertures) could be used for studying the influence of box geometry and tested boundary conditions on the limit resistance to pullout. Due to the direct contribution of transverse ribs, it is possible that the influence of friction of backfill and side walls, and the influence of geogrid width as related to box width, will be different from the influence determined with wire mesh modelled by membrane element or 3D volumetric element. This type of study is conducted in this paper, as elaborated in full detail in Section 4.

#### 4. New model and results of numerical 2D and 3D simulations

As a particular emphasis is placed in this paper on the influence of boundary conditions on the resistance at pullout, an appropriate set of 2D and 3D simulations of actual tests was developed [93] to determine the influence of side wall friction on the equivalent coefficient of friction.

The new numerical model is presented in detail in Figure 8. This model of wire mesh reinforcement is composed of transverse and longitudinal ribs. Transverse ribs are modelled with beam elements whose height is equal to the transverse rib diameter, while longitudinal ribs are modelled with the truss element that links individual transverse ribs. The proposed grid-reinforcement model is relatively simple as the total resistance to pullout is reduced to the passive resistance of backfill in front of transverse ribs, while the friction and the contact between the backfill and transverse ribs is neglected. This assumption is justified by the results of experimental research, according to which transverse ribs contribute to the total mobilised resistance to pullout of wire mesh reinforcement much more than longitudinal ribs (over 90%, [40]).

Based on detailed sensitivity analyses [93], the following details of the numerical model, relating to the study of the influence of boundary conditions on results, were adopted:

- Extremely small average dimensions of finite elements were adopted, which is based on criteria that it should be verified for every analysed model that further increase of density does not influence results by more than 1% as related to the previous density level (2D model – Figure 8.a), i.e. that maximum capacities of the program are used as to number of elements (3D model – Figure 8.b),
- The refined finite element mesh was used in the zone around transverse ribs (as the result is greatly influenced by density in this zone), while lower density was used in the zone situated further apart from transverse ribs. This enabled significant savings as to the duration of computations/analyses, with a negligible influence on the result.

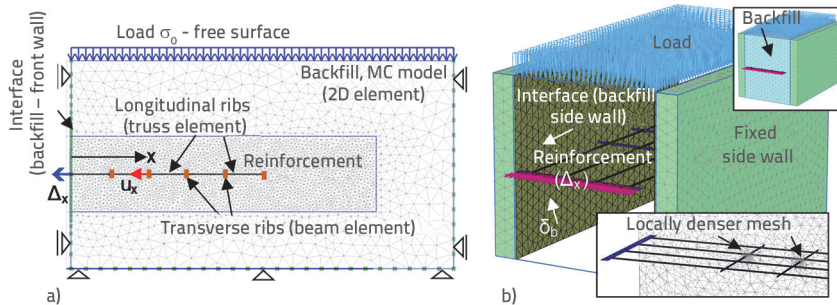


Figure 8. New numerical model of pullout test for wire mesh reinforcement: a) 2D model; b) 3D model [92]

- Triangular finite elements with 15 nodes and 12 integrated Gaussian points were applied during numerical 2D simulation of the pullout test. A finite element in the form of a tetrahedron, with 10 nodes and 4 integration points, was used in 3D analyses.
- As similar limit pullout force values were obtained for similar strength parameters by the Mohr-Coulomb and Hardening Soil models, the Mohr-Coulomb constitutive model was applied in further analysis.
- Pullout modelling with imposed displacement was selected in this paper for pullout simulation, as the difference is quite small between pullout simulation by imposed force or by imposed displacement at the front end of wire mesh reinforcement.
- Results of sensitivity analyses show that the top and bottom limits of the horizontal pressure coefficient at rest ranging from 0.2 to 1.0 exhibit practically the same mobilisation of resistance at pullout as in the case of initial stress modelling using expression proposed by Jaky [106].
- The influence of the position of the back and bottom box walls on limit resistance is negligible in comparison with the position of the front and top walls. For this reason, special attention was paid to the study of the influence of backfill height above wire mesh reinforcement on the bearing capacity at the pullout.
- The analysis involving greater deformation was applied, as a difference exists between simulation results with and

without analysis of large deformations (updated Lagrange formulation).

Numerical simulation results were compared with published experiments [30, 39] and analytical solutions based on the principles of limit equilibrium. It has been demonstrated that the new numerical model successfully describes load transfer mechanisms determined by microlevel measurements and that the global response of the model is in accordance with published measurement results [93].

After the mentioned optimisation and verification of the new model, several additional pullout test simulations were made (144 for 2D model and 11 for 3D model) to determine the influence of boundary conditions and geometry of wire mesh reinforcement on the ultimate resistance at the pullout. Models differ from one another by the level of backfill above the reinforcement ( $H$ ), mesh reinforcement geometry ( $S/t$  and  $L_s$ ), position of reinforcement in the box ( $x_1$ ), compaction of backfill (defined by the angle of internal friction, dilation angle, and elastic modulus), backfill and box wall friction ( $\delta_p = 0^\circ; 6^\circ$  and  $25^\circ$ ), and the ratio of box width to mesh reinforcement width ( $B_s/B$ ). Individual values are shown in Figure 9 and earlier in Figure 2, while geotechnical parameters of backfill are given in Table 2.

In all simulations, the load exerted on the surface of backfill material was selected in such way that the initial vertical effective stress is at the geogrid level  $\gamma \cdot H + \sigma_0 = 40.0 \text{ kPa}$  (corresponds to the depth of approximately 2.0 m below the top of the wall, where the probability of pullout is the highest in a real-life wall). The steel wire mesh reinforcement with the transverse and longitudinal ribs measuring 5.0 mm in diameter was used in all analyses. Such – relatively stiff – inelastic wire mesh reinforcement prevented failure of reinforcement due to exceedance of tensile stress, and is therefore considered suitable for the conduct of pullout tests.

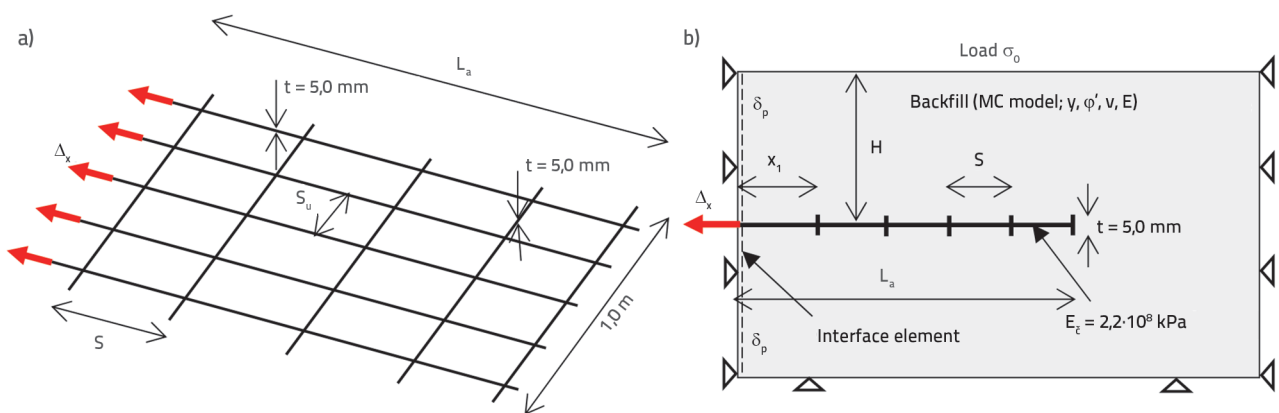


Figure 9. Presentation of individual values: a) geometrical properties of wire mesh reinforcement and b) test setup and notation

Table 2. Geotechnical properties of backfill material

Parameter, symbol, unit	Loose backfill	Dense backfill
Unit weight, $\gamma$ [kN/m <sup>3</sup> ]	17.0	17.0
Effective angle of internal friction, $\phi'$ [°]	31.0	44.0
Dilation angle, $\psi$ [°]	3.0	11.0
Effective cohesion, $c'$ [kN/m <sup>2</sup> ]	0.01	0.01
Reference elastic modulus, $E_{ref}$ [kN/m <sup>2</sup> ]	10000.0	50000.0
Poisson ratio, $\nu$ -	0.3	0.3

Typical 2D simulation results are presented in Figure 10 where the influence of backfill density on the increase in resistance to pullout is shown (Figure 10.a). As expected, greater compaction results in greater pullout force and faster mobilisation of resistance ( $F_p$ ) with and increase of imposed displacement at the front end of wire mesh reinforcement ( $\Delta_x$ ). The zone of maximum increment of shear strain at limit displacement (Figure 10.b) points to the failure mechanism of backfill due to pullout. In case of dense backfill, this failure is caused by attainment of limit passive resistance in front of all transverse ribs, which causes formation of two failure surfaces (under and above the geogrid level). These two surfaces spread toward the front wall of the box, which results in mobilisation of friction at the interface between the backfill and this wall. The failure zone defined by maximum shear strain increments is localised for loose backfill around transverse ribs, and so backfill displacements at greater distance from wire mesh reinforcement are considerably lower than in case of dense backfill.

That is why the influence of boundary conditions on geogrid pullout test results are considerably lower in case of loose backfill compared to dense backfill. As compacted granular backfill – rather than loose backfill - is normally used for walls made of reinforced earth, only the case of dense backfill will be analysed during the investigation of the influence of boundary conditions on test results.

The influence of friction at the front wall on the equivalent coefficient of friction for dense backfill and wire mesh reinforcement is shown in Figure 11. In accordance with the result shown in Figure 10.b, and the related interpretation, greater friction at the front wall results in an increase in resistance to pullout (i.e. in an increase of equivalent coefficient of friction,  $f^*$ ).

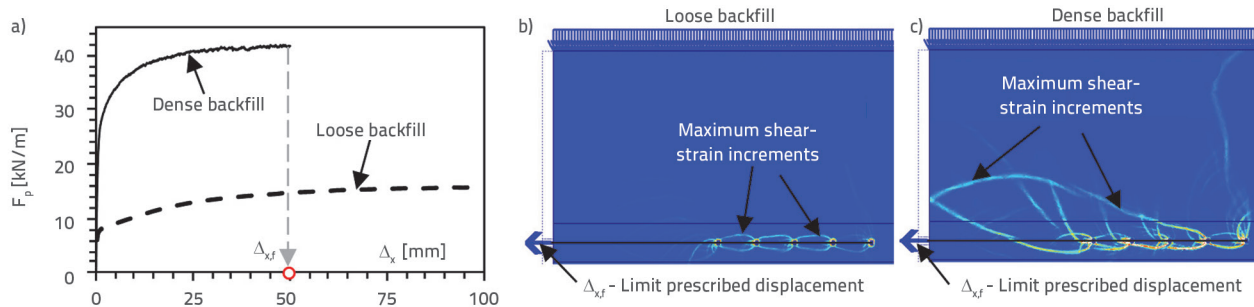


Figure 10. Influence of backfill compaction on typical simulation result: a) force-displacement dependence; b) pullout mechanism for loose backfill; c) pullout mechanism for dense backfill

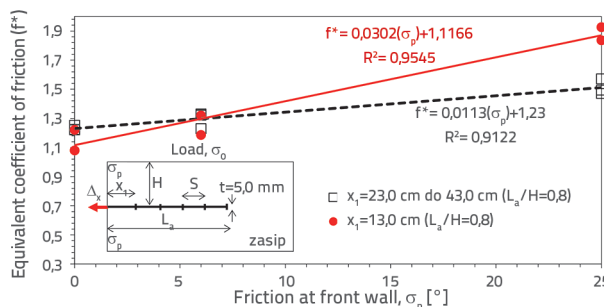


Figure 11. Influence of friction at the front wall on the equivalent coefficient of friction [93]

The influence of friction reduces considerably with an increase in the distance of the first transverse rib from the front wall, which points to a less steep positioning of the regression line determined for the case of distance,  $x_1 = 23.0$  cm, as compared to the distance,  $x_1 = 13.0$  cm. In the case of loose backfill, this influence is practically negligible as the backfill failure occurs only locally in such material, and does not greatly mobilise the mass of the backfill. These results are in accordance with experiments in which the size of backfill zone around geogrid is determined through transparent glass. In such experiments, the said zone moves during pullout imposed at the front end [33].

Figure 12 shows the influence of the ratio of wire mesh reinforcement length to backfill height above the reinforcement level ( $L_a/H$ ) on the equivalent coefficient of friction ( $f^*$ ) of dense backfill and reinforcement. The results are related to the model with an ideally smooth front wall, and with the ratio of distance to diameter of transverse ribs ( $S/t$ ) that amounts to 20.0 and 40.0. The use of wire mesh reinforcement that is short as compared to overburden height (e.g.  $L_a/H = 0.75$ , Figure 12.b) results in a different failure mechanism, and in a more significant influence of boundary conditions on simulation results as related to the case of geometric configurations with greater ratio of wire mesh reinforcement length to overburden height (e.g.  $L_a/H = 4.15$ , Figure 12.b). Because of different pullout mechanism, in case of lower  $L_a/H$  ratios (shorter wire mesh reinforcement – Figure 12.c), one can observe an increase in average normal stress at the level of reinforcement ( $\sigma_n$ ) at limit displacement as compared to the initial one,  $\gamma H + \sigma_v$ , and hence the interpreted value of the equivalent coefficient of friction ( $f^*$ ) is considerably higher than in the case when the slip surface does not attain the front edge (Figure 12.b).

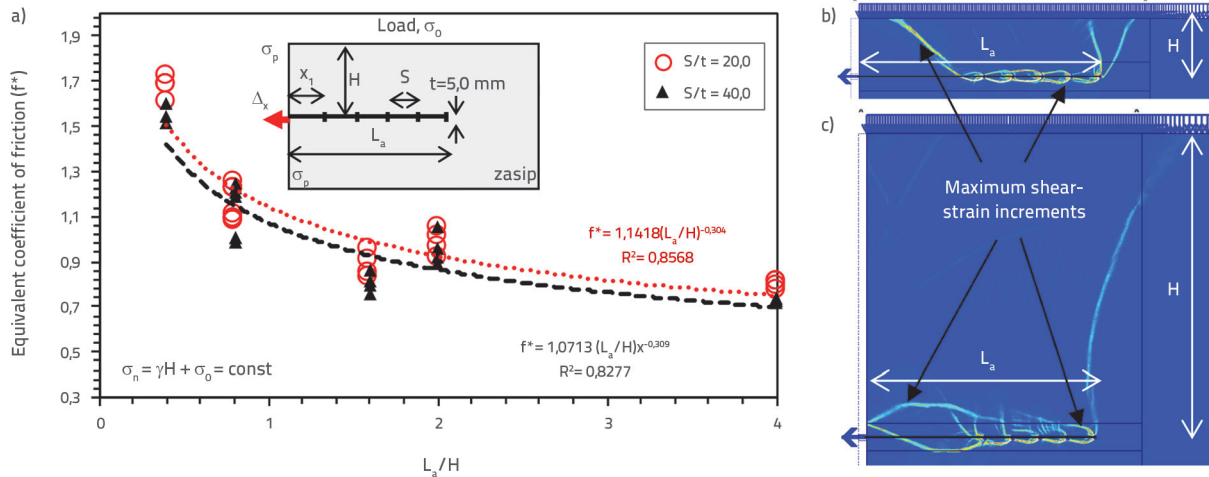


Figure 12. Influence of the ratio of wire mesh reinforcement length to backfill height above reinforcement level ( $L_a/H$ ) on the equivalent coefficient of friction ( $F$ ); b) pullout mechanism for  $L_a/H = 4.15$ ; c) pullout mechanism for  $L_a/H = 0.75$  [93]

Figure 13 shows vertical stress diagrams at the interface between wire mesh reinforcement and backfill (the cross section is 5.0 mm above the geogrid level) at limit pullout force.

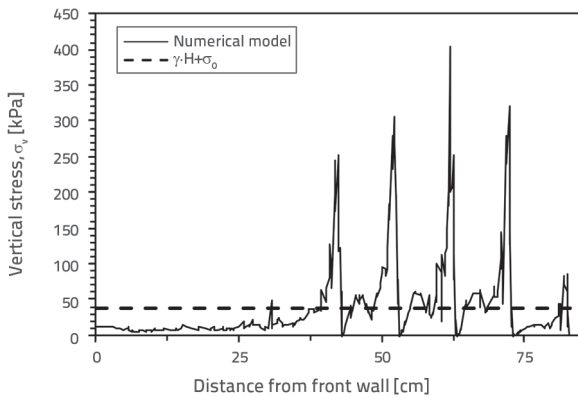


Figure 13. Distribution of normal stress at limit pullout force, 5.0 mm above the geogrid level

The results show that numerical model can describe stress distribution determined during tests (e.g. [24]), which differs from the assumption that normal stress at wire mesh reinforcement level is constant during the test. According to these results, an average vertical stress along the entire length of the box corresponds to the value of  $\gamma \cdot H + \sigma_o$ , although an average stress along the geogrid length is greater due to influence of transverse ribs and boundary conditions. Considerable increase in vertical stress occurs in the zone in front of transverse ribs and, at that, this stress behind ribs practically falls to zero but only to increase toward the following transverse rib (Figure 13). The determined trend shows that the equivalent coefficient of friction remains practically constant in case of ratios of  $L_a/H > 1.5$ . The use of wire mesh reinforcement that is relatively short compared to the height of backfill above it ( $L_a/H < 1.5$ ) results in equivalent coefficients of friction that are greater than the tangent of the angle of internal friction in the case of the use of conventional assumption stipulating that normal stress at the geogrid level remains constant from the start to the end of pullout test ( $\gamma \cdot H + \sigma_o = \text{const}$ ). By eliminating the influence of

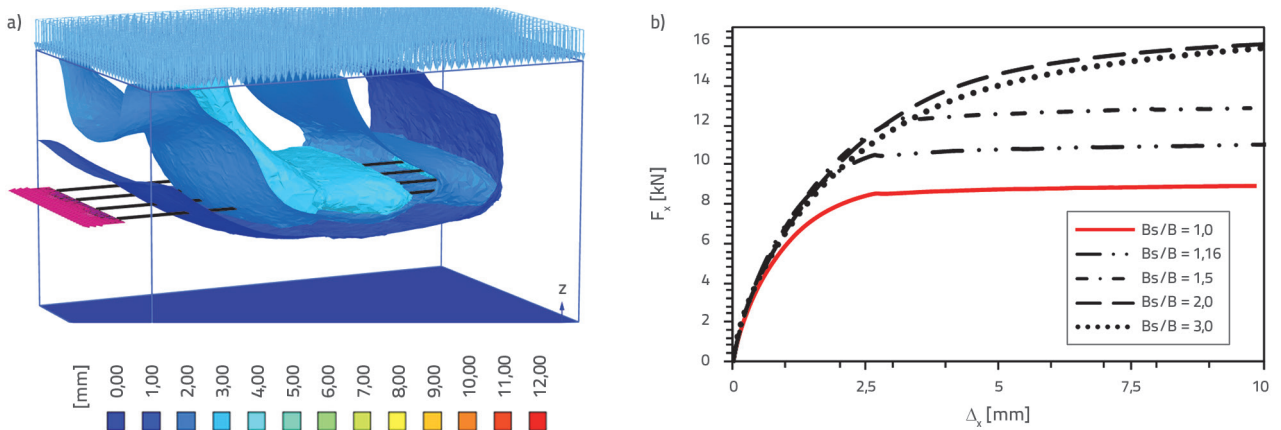


Figure 14. a) total backfill displacements at limit pullout force for wire mesh reinforcement  $B_s/B = 1,5$ ; b) Influence of box width (at constant wire mesh reinforcement width) on limit resistance at pullout

**Table 3. Influence of side wall lubrication (simulated by reduction of friction at the wall and backfill interface) and backfill compaction on the limit resistance at pullout determined by 3D model**

Backfill and friction $B_s/B = 1,16$	Dense backfill			Loose backfill		
	$\delta_b = 3^\circ$	$\delta_b = 6^\circ$	$\delta_b = 25^\circ$	$\delta_b = 3^\circ$	$\delta_b = 6^\circ$	$\delta_b = 25^\circ$
$F_{p,ult}$ [kN]	10.8	11.3	17.2	5.7	5.9	8.2

boundary conditions, i.e. by placing wire mesh reinforcement further away from the front wall, and by using sufficiently low height of backfill as related to reinforcement length, the realised equivalent coefficients of friction become lower or equal to the tangent of the angle of internal friction of backfill (for the analysed cases of backfill material).

Three-dimensional numerical simulations were used to analyse the influence of wire mesh reinforcement width and side wall friction on test results. As the influence of the backfill and front wall friction was thoroughly investigated through 2D analyses, this wall is modelled in all 3D analyses as an ideally smooth wall. The case of wire mesh reinforcement with three transverse ribs installed in dense backfill was analysed at vertical load of 30.0 kPa, all in accordance with Figure 8. The constant reinforcement width of 30.0 cm was used in combination with the box width of 30.0; 35.0; 45.0; 60.0 and 90.0 cm, which defined the ratio of the pullout box width to reinforcement width ( $B_s/B$ ) of 1.0; 1.16; 1.5; 2.0 and 3.0. Numerical simulation results are presented in Figure 14. Figure 14.a shows total backfill displacements around wire mesh reinforcement at limit pullout force, while the dependence of force and displacement at the front end of reinforcement is shown in Figure 14.b. The results show that the use of wire mesh reinforcement that is narrower than the box results in an increase of pullout force, which is in accordance with experimental research conducted with geogrids [46].

In addition, it was demonstrated that the use of wire mesh reinforcement that is not much narrower in width than the box (box and reinforcement width ratio,  $B_s/B = 1,16$ ), with the „lubrication“ of side walls (simulated by model through strength reduction at this contact), greatly reduces the influence of friction between the backfill and these surfaces. It can also be seen that reduction of friction results, already at  $\delta_b = 6^\circ$ , in the state of stress that corresponds to the practically ideally smooth side wall (Table 3). Two basic trends can be differentiated based on 3D analysis results:

- Side wall friction greatly influences limit resistance at the pullout of wire mesh reinforcement from a relatively narrow box,
- Contribution of side wall friction to the increase in limit resistance is greater in the case of dense backfill compared to loose backfill.

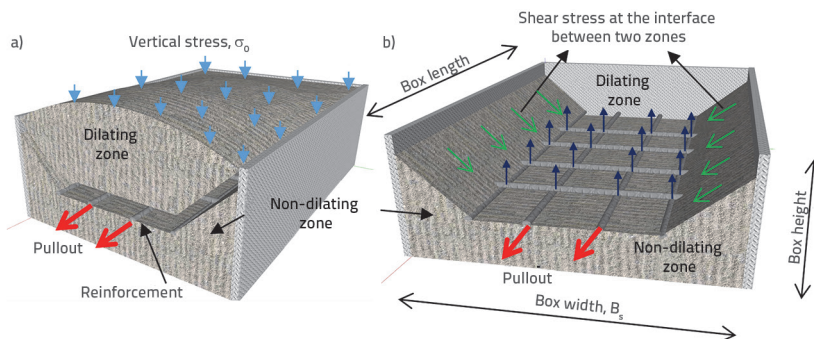


**Figure 15. 3D effect at pullout of grid narrower than the box: a) deformed configuration of backfill; b) shear stress at the limit of dilating and non-dilating zones of backfill [93]**

These trends are in accordance with experimental research [46], which points to pullout test deficiencies in case the test is performed with geogrid that is much narrower than the box. Results obtained by 3D model in which geogrid is narrower than the box are shown in Figure 15. Two typical backfill zones are formed during pullout: top dilating zone (above the geogrid – displacements oriented vertically toward the top of the box) and the bottom non-dilating zone (under the geogrid) in which backfill material exhibits low level of deformation. Shear stress can be noted at the interface of these two zones, as shown in Figure 15.b. This stress component increases normal stress at side edges of wire mesh reinforcement/geogrid. This causes an increase in pullout resistance as compared to the case when this effect does not exist (i.e. when the wire mesh reinforcement width is equal to the box width), which has also been registered earlier in the case of strip shaped geosynthetics [24]. As wire mesh reinforcements, unlike geosynthetic/steel strips, are most often realized in walls in such a way that they cover the entire surface, this effect should be reduced at grid pullout test by using geogrids that are not narrower than the box, and by lubrication of side walls of the box before the backfill is placed.

### 5. Conclusion

Numerical modelling can enable better understanding of interaction mechanisms during realisation of pullout tests, and can also assist in the elaboration of recommendations about realisation of pullout tests. Numerical simulations of the pullout of various geometrical grid-reinforcement configurations from various types of backfill material have been used to improve the understanding of interaction mechanisms in pullout test conditions.

- Based on an overview of simulations published so far in the literature, numerical models of the pullout of geogrid/wire mesh reinforcement from cohesionless backfill material can be classified into four basic groups:
- test models with wire mesh reinforcement/geogrid as a equivalent cable element of unit width ("geogrid" element),
- test models with wire mesh reinforcement/geogrid that is composed of longitudinal ribs simulated by cable element of unit width and transverse ribs modelled as beams of real thickness,
- test models with wire mesh reinforcement/geogrid that is composed of transverse ribs only,
- test models with three-dimensional wire mesh reinforcement/geogrid.

Numerical models that simulate pullout resistance of transverse ribs, or longitudinal and transverse ribs taken individually, successfully describe behaviour registered during the corresponding tests [28, 37, 40, 88]. These numerical models can adequately describe dependence between force and displacement, and hence they can predict equivalent friction at the contact between wire mesh reinforcement/geogrid and backfill that is used during traditional calculations of internal stability of walls made of reinforced earth. Influences of individual elements determined by physical tests presented by Moraci et al. [25] do not practically differ from trends shown in numerical analyses presented in this paper.

- Numerical simulations conducted in the scope of this paper show that pullout test results are mostly influenced by:
- ratio of backfill height above the geogrid (H) to wire mesh reinforcement length (measured from front wall –  $L_a$ ),
- backfill and box wall friction (dominant at the front wall, but considerable at side walls).

A wide spectrum of geometrical configurations of wire mesh reinforcements and boxes is analysed in the paper. Based on results obtained by numerical analyses, with all limitations these analyses bring, recommendations are given about the realisation of pullout tests. More specifically, boxes for the pullout of wire mesh reinforcement/geogrid from dense granular material should be designed in the following way, to eliminate the influence of boundary condition on test results:

- use sleeves more than 20.0 cm in length, which is in accordance with EN and ASTM standards,
- use smaller backfill heights above wire mesh reinforcement (H) as compared to geogrid length ( $L_a$ ). More specifically, the ratio should be  $L_a/H > 1.5$ , with the respect of ASTM and EN standards related to the required box height as a function of grain size of backfill material.
- wire mesh reinforcement should be placed close to side walls and, before the backfill is placed, box walls should be lubricated in order to reduce friction at the interface with backfill (this especially concerns front walls and side walls). Box wall preparation rules are defined in the corresponding ASTM standard.

These recommendations on the realisation of tests are based on numerical analyses conducted by the authors, and they also relate to the properties of materials and conditions in which they were used. The recommendations must also be considered in the light of limitations inherent to numerical analyses, and can not, therefore, be generalized. In any case, recommendations for improvement of test procedure should also be considered from the perspective of experience gained during realisation of these tests.

## REFERENCES

- [1] Anderson, P.L., Gladstone, R.A., Withiam, J.L.: Coherent gravity: The correct design method for steel-reinforced MSE wall, Earth Retention Conference 3, pp. 512-521, 2010.
- [2] Choudhary, A.K., Krishna, A.M.: Experimental investigation of interface behaviour of different types of granular soil/geosynthetics, International Journal of Geosynthetics and Ground Engineering, 2 (2016) 1, pp. 1-11.
- [3] Holtz, R.D.: 46<sup>th</sup> Terzaghi Lecture: Geosynthetic Reinforced Soil: From the Experimental to the Familiar, Journal of Geotechnical and Geoenvironmental Engineering, 143 (2017) 9, [https://doi.org/10.1061/\(ASCE\)GT.1943-5606.0001674](https://doi.org/10.1061/(ASCE)GT.1943-5606.0001674)
- [4] Christopher, B.R., Gill, S.A., Giroud, J.P., Juran, I., Mitchell, J.K., Schlosser, F., Dunncliff, J.: Reinforced soil structures Volume I. Design and construction guidelines, No. FHWA-RD-89-043, 1 (1990).
- [5] Koerner, R.M.: Designing with Geosynthetics 4<sup>th</sup> Edition, Prentice Hall, pp. 761, 2008.
- [6] Ingold, T.S.: Laboratory pull-out testing of grid reinforcements in sand, ASTM geotechnical testing journal, 61 (1983) 3, pp. 101-111.
- [7] Ochiai, H., Hayashi, S., Otani, J., Umezaki, T., Ogisako, E.: Field pullout test of polymer grid in embankment, Proceedings of the International Interaction between soil and grid reinforcements, pp. 349, 1998.
- [8] Johnston, R.S., Romstad, K.M.: Dilation and boundary effects in large scale pull-out tests, 12<sup>th</sup> International Conference on Soil Mechanics and Foundation Engineering, Rio De Janeiro, Brasil, pp. 1263-1266, 1989.
- [9] Palmeria, E.M., Milligan, G.W.E.: Scale and other factors affecting the results of pull-out tests of grids buried in sand, Geotechnique, 39 (1989) 3, pp. 511-542.
- [10] Muthu, R.D.: Large scale pullout testing of geosynthetics, Master Thesis, 1991.
- [11] Ochiai, H., Hayashi, S., Otani, J., Hirai, T.: Evaluation of pull-out resistance of geogrid reinforced soils, Proceedings of Earth Reinforcement Practice, pp. 146, 1992.
- [12] Ochiai, H., Otani, J., Hayashic, S., Hirai, T.: The Pull-Out Resistance of Geogrids in Reinforced Soil, Geotextiles and Geomembranes, 14 (1996), pp. 19-42.

- [13] Farrag, K., Acar, Y.B., Juran, I.: Pull-out resistance of geogrid reinforcements, *Geotextiles and Geomembranes*, 12 (1993) 2, pp. 133-159.
- [14] Bergado, D.T., Lo, K.H., Chai, J.C., Shivashankar, R., Alfaro, M.C., Anderson, L.R.: Pullout tests using steel grid reinforcements with low-quality backfill, *Journal of Geotechnical Engineering ASCE USA*, 118 (1992) 7, pp. 1047-1063.
- [15] Bergado, D.T., Chai, J.C.: Pullout force/displacement relationship of extensible grid reinforcements, *Geotextiles and geomembranes*, 13 (1994) 5, pp. 295-316.
- [16] Alfaro, M.C., Miura, N., Bergado, D.T.: Soil-geogrid reinforcement interaction by pullout and direct shear tests, 1995.
- [17] Lopes, L.M., Ladeira, M.: Influence of Confinement, Soil Density and displacement rate on Soil-Geogrid interaction, *Geotextiles and Geomembranes*, 14 (1996), pp. 543-554.
- [18] Farrag, K., Morvant, M.: Effect of clamping mechanism on pullout and confined extension tests, Grips, Clamps, Clamping Techniques, and Strain Measurement for Testing of Geosynthetics, ASTM International, 2000.
- [19] Chang, D.T., Chang, F.C., Yang, G.S., Yan, C.Y.: The influence factors study for geogrid pullout test, Grips, Clamps, Clamping Techniques, and Strain Measurement for Testing of Geosynthetics, ASTM International, 2000.
- [20] Bolt, A.F., Duszyńska, A.: Pull-out testing of geogrid reinforcements, 2nd European Conference on Geosynthetics, Bologna, Italy, 2000.
- [21] Sugimoto, M., Alagiyawanna, A.M.N., Kadoguchi, K.: Influence of rigid and flexible face on geogrid pullout tests, *Geotextiles and Geomembranes*, 19 (2000) 5, pp. 257-277.
- [22] Perkins, S.W., Edens, M.Q.: Finite element modeling of a geosynthetic pullout test, *Geotechnical and Geological Engineering* 21 (2003), pp. 357-375.
- [23] Nejad, F.M., Small, J.C.: Pullout behaviour of geogrids, *Iranian Journal of Science & Technology, Transaction B, Engineering*, 29 (2003) 3, pp. 301-310.
- [24] Alfaro, M.C., Pathak, Y.P.: Dilatant stresses at the interface of granular fills and geogrid strip reinforcements, *Geosynthetics International*, 12 (2005), pp. 239-252.
- [25] Moraci, N., Recalcati, P.: Factors affecting the pullout behaviour of extruded geogrids embedded in a compacted granular soil, *Geotextiles and Geomembranes*, 24 (2006), pp. 220-242.
- [26] Teixeira, S.H., Bueno, B.S., Zornberg, J.G.: Pullout resistance of individual longitudinal and transverse geogrid ribs, *Journal of geotechnical and geoenvironmental engineering*, 133 (2007), pp. 37-50.
- [27] Abdel-Rahman, A.H., Ibrahim, M.A.M., Ashmawy, A.K.: Utilization of a Large-Scale Testing Apparatus in Investigating and Formulating the Soil/Geogrid Interface Characteristics in Reinforced Soils, *Australian Journal of Basic and Applied Sciences*, 1 (2007) 4, pp. 415-430.
- [28] Khedkar, M.S., Mandal, J.N.: Pullout behaviour of cellular reinforcements, *Geotextiles and Geomembranes*, 27 (2009), pp. 262-271.
- [29] Liao, X., Ye, G., Xu, C.: Friction and Passive Resistance of Geogrid in Pullout Tests, *ASCE Advances in Ground Improvement: GSP*, 188 (2009), pp. 252-259.
- [30] Minažek, K.: Modelsko Ispitivanje interakcije geomreže i tla, Doktorska disertacija, Sveučilište u Zagrebu, Građevinski fakultet, 2010.
- [31] Fan, C.C., Hsieh, C.C.: The mechanical behaviour and design concerns for a hybrid reinforced earth embankment built in limited width adjacent to a slope, *Computers and Geotechnics*, 38 (2011) 2, pp. 233-247.
- [32] Dechakulsom, M., Sukolrat, J., Sawangsuriya, A.: Behavior of a Trial Embankment with Reinforced Steep Slope and Mechanically Stabilized Earth Wall: A Numerical Analysis, *Proceedings of Geo-Frontiers: Advances in Geotechnical Engineering*, 2011.
- [33] Zhou, J., Chen, J.F., Xue, J.F., Wang J.Q.: Micro-mechanism of the interaction between sand and geogrid transverse ribs, *Geosynthetics International*, 19 (2012) 6.
- [34] Suksiripattanapong, C., Horpibulsuk, S., Chinkulkijniwat, A., Chai, J.C.: Pullout resistance of bearing reinforcement embedded in coarse-grained soils, *Geotextiles and Geomembranes*, 36 (2013), pp. 44-54.
- [35] Minažek, K., Mulabdić, M.: Pregled ispitivanja interakcije tla i armature u armiranom tlu pokusom izvlačenja, *Građevinar*, 65 (2013), pp. 235-250.
- [36] Lajevardi, S.H., Dias, D., Racinais, J.: Analysis of soil-welded steel mesh reinforcement interface interaction by pull-out tests, *Geotextiles and Geomembranes*, 40 (2013), pp. 48-57.
- [37] Abdi, M.R., Zandieh, A.R.: Experimental and numerical analysis of large scale pull out tests conducted on clays reinforced with geogrids encapsulated with coarse material, *Geotextiles and Geomembranes*, 42 (2014) 5, pp. 494-504.
- [38] Jayawickrama, P.W., Lawson, W.D., Wood, T.A., Surlis, J.G.: Pullout Behavior of Welded Grid Reinforcements Embedded in Coarse Granular Backfill, *Geo-Congress Technical Papers@ sGeo-characterization and Modeling for Sustainability*, pp. 2558-2567, 2014.
- [39] Alam, M.J.I.: Pull-out behaviour of steel grid soil reinforcement in silty sand, Masters by Research Thesis, 2012.
- [40] Alam, M.J.I., Lo, S.R., Karim, M.R.: Pull-out behaviour of steel grid soil reinforcement embedded in silty sand, *Computers and Geotechnics*, 56 (2014), pp. 216-226.
- [41] Touahmia, M.: Interaction mechanisms of soil-geosynthetic reinforcement, *International Journal of GEOMATE*, 7 (2014) 13, pp. 969-973.
- [42] Mosallanezhad, M., Bazayr, M.H., Saboor, M.H.: Novel strip-anchor for pull-out resistance in cohesionless soils, *Measurement*, 62 (2015), pp. 187-196.
- [43] Ferreira, J.A., Zornberg, J.G.: A transparent pullout testing device for 3D evaluation of soil-geogrid interaction, 2015.
- [44] Ferreira, F.B., Vieira, C.S., Lopes, M.L., Carlos, D.M.: Experimental investigation on the pullout behaviour of geosynthetics embedded in a granite residual soil, *European Journal of Environmental and Civil Engineering*, 20 (2016) 9, pp. 1147-1180.
- [45] Sadat Taghavi, S.H., Mosallanezhad, M.: Experimental analysis of large-scale pullout tests conducted on polyester anchored geogrid reinforcement systems, *Canadian Geotechnical Journal*, 999 (2016), pp. 1-10.
- [46] Moraci, N., Cardile, G., Giofrè, D., Mandaglio, M.C., Calvarano, L.S., Carbone, L.: Soil geosynthetic interaction: design parameters from experimental and theoretical analysis, *Transportation Infrastructure Geotechnology*, 1 (2014) 2, pp. 165-227.
- [47] Karpurapu, R., Bathurst, R.J.: Behaviour of geosynthetic reinforced soil retaining walls using the finite element method, *Computers and Geotechnics*, 17 (1995) 3, pp. 279-299.
- [48] Ho, S.K., Rowe, R.K.: Effect of wall geometry on the behaviour of reinforced soil walls, *Geotextiles and Geomembranes*, 14 (1996) 10, pp. 521-541.
- [49] Carrubba, P., Moraci, N., Montanelli, F.: Instrumented soil reinforced retaining wall: analysis of measurements, *Geosynthetics' 99 Conference Proceedings*, pp. 921-934, 1999.

- [50] Hashimoto, H.: Finite element study of a geosynthetic-reinforced soil retaining wall with concrete-block facing, *Geosynthetics International*, 7 (2000) 2, pp. 137.
- [51] Leshchinsky, D., Vulova, C.: Numerical investigation of the effects of geosynthetic spacing on failure mechanisms in mechanically stabilized earth block walls, *Geosynthetics International*, 8 (2001) 4, pp. 343–365.
- [52] Hatami, K., Bathurst, R.J.: Development and verification of a numerical model for the analysis of geosynthetic-reinforced soil segmental walls under working stress conditions, *Canadian Geotechnical Journal*, 42 (2005) 4, pp. 1066-1085.
- [53] Stanić, B., Kovačević, M.S., Szavits-Nossan, V.: Assessment of deformations of a reinforced soil structure, *Proc. XIIIth European Conference on Soil Mechanics And Geotechnical Engineering*, pp. 887-892, 2000.
- [54] Guler, E., Hamderi, M., Demirkan, M.M.: Numerical analysis of reinforced soil-retaining wall structures with cohesive and granular backfills, *Geosynthetics International*, 14 (2007) 6, pp. 330–345.
- [55] Abioghli, H.: Effect of Changes of Mesh Size on the Numerical Analysis of Reinforced Soil Walls, *Australian Journal of Basic and Applied Sciences*, 5 (2011) 12, pp. 1693-1696.
- [56] Liu, H.: Long-term lateral displacement of geosynthetic-reinforced soil segmental retaining walls, *Geotextiles and Geomembranes*, 32 (2012), pp. 18-27.
- [57] Skejic, A., Balic, A., Jasarevic, H., Namas, T., Selman, S., Karamehmedovic, E., Bucu, J.: Observation and Numerical Modeling of Test MSEW with Inextensible Inclusions and Coarse Crushed Stone Backfill, *The Electronic Journal of Geotechnical Engineering*, 18 (2013), pp. 2878–2892.
- [58] Damians, I.P., Bathurst, R.J., Josa, A., Lloret, A.: Numerical Analysis of an Instrumented Steel-Reinforced Soil Wall, *International Journal of Geomechanics*, (2014).
- [59] Yu, Y., Bathurst, R.J., Allen, T.M.: Numerical modelling of two full-scale reinforced soil wrapped-face walls, *Geotextiles and Geomembranes*, (2017).
- [60] Skejic, A., Medic, S., Dolarevic, S.: Influence of wire mesh characteristics on reinforced soil model wall failure mechanisms-physical and numerical modelling, *Geotextiles and Geomembranes*, 46 (2018), pp. 726–738.
- [61] Ling, H.I., Leshchinsky, D., Tatsuoka, F.: *Reinforced soil engineering: advances in research and practice*, CRC Press, 2003.
- [62] Rowe, R.K., Skinner, G.D.: Numerical analysis of geosynthetic reinforced retaining wall constructed on a layered soil foundation, *Geotextiles and geomembranes*, 19 (2001) 7, pp. 387-412.
- [63] Holtz, R.D., Lee, W.F.: *Internal stability analyses of geosynthetic reinforced retaining walls*, No. WA-RD 532.1., Olympia, Washington, Washington State Department of Transportation, 2002.
- [64] Bergado, D.T., Youwai, S., Teerawattanasuk, C., Visudmedanukul, P.: The interaction mechanism and behavior of hexagonal wire mesh reinforced embankment with silty sand backfill on soft clay, *Computers and Geotechnics*, 30 (2003), pp. 517–534.
- [65] Suksiripattanapong, C., Chinkulkijniwat, A., Horpibulsuk, S., Rujikiatkamjorn, C., Tanhsutthinon, T.: Numerical analysis of bearing reinforcement earth (BRE) wall, *Geotextiles and Geomembranes*, 32 (2012), pp. 28-37.
- [66] Palmeira, E.M.: *The study of soil-reinforcement interaction by means of largescale laboratory tests*, Doctoral dissertation, University of Oxford, 1987.
- [67] Montanelli, F., Recalcati, P.: Geogrid reinforced railways embankments: design concepts and experimental test results, *International Association for Bridge and Structural Engineering, IABSE Symposium Report*, 87 (2003) 6, pp.1-9.
- [68] Palmeira, E.M., Milligan, G.W.: Large scale direct shear tests on reinforced soil, *Soils and foundations*, 29 (1989) 1, pp. 18-30.
- [69] Lawson, W.D., Jayawickrama, P.W., Wood, T.A., Surles, J.G.: Pullout resistance factors for steel reinforcements used in TxDOT MSE walls, *Geo-Congress 2013: Stability and Performance of Slopes and Embankments III*, pp. 44-53, 2013.
- [70] ASTM D6706 – 01: Standard Test Method for Measuring Geosynthetic Pullout Resistance in Soil, *ASTM International*, 2007.
- [71] Technical Committee CEN/TC 189: EN 13738 Geotextiles and geotextile-related products - Determination of pullout resistance in soil, *European committee for standardization, Technical Committee CEN/TC 189, Brussels, Belgium*, 2004.
- [72] Merellec, P.: *Reinforced Earth-earch/reinforcement bond*, Thesis, 1977.
- [73] Chang, J.C., Hannon, J.B., Forsyth, R.A.: Pull resistance and interaction of earthwork reinforcement and soil, *Transportation Research Record*, pp. 640, 1977.
- [74] Alimi, I., Bacot, J., Lareal, P., Schlosser, F., Long, N.: In-situ and laboratory study of the adhesion between soil and reinforcement, *Bull Liaison lab ponts chauss, Spec. VI-E*, 1978.
- [75] Dyer, M.R.: *Observation of the stress distribution in crushed glass with applications to soil reinforcement*, Doctoral dissertation, University of Oxford, 1985.
- [76] Bauer, G.E., Mowafy, Y.M.: The interaction mechanism of granular soils with geogrids, *International Conference on Numerical Methods in Geomechanics*, 6. Innsbruck Proceedings, Innsbruck, Swoboda, Balkema, Rotterdam, 2 (1988), pp. 1263-1272.
- [77] Sugimoto, M., Alagiyawanna, A.M.N.: Pullout Behavior of Geogrid by Test and Numerical Analysis, *Journal Of Geotechnical and Geoenvironmental Engineering © ASCE*, 4 (2003), pp. 361-371.
- [78] Jewell R.A., Miligan G.W.E., Sarsby R.W., Dubois D.: Interaction between soil and geogrids, *Proceedings of the Symposium on Polymer Grid Reinforcement in Civil Engineering*, London, Thomas Telford, pp. 19–29, 1984.
- [79] Yogarajah, I., Yeo, K.C.: Finite element modelling of pull-out tests with load and strain measurements. *Geotextiles and Geomembranes*, 13 (1994) 1, pp. 43–54., [https://doi.org/10.1016/0266-1144\(94\)90056-6](https://doi.org/10.1016/0266-1144(94)90056-6)
- [80] Wilson-Fahmy, Koerner R.: Finite Element Modelling of Soil-Geogrid Interaction with Application to the Behavior of Geogrids in a Pullout Loading Condition, *Geotextiles and Geomembranes*, 12 (1993), pp. 479-501.
- [81] Alobaidi, I. A., Hoare, D.J., Ghataora, G.S.: Load transfer mechanism in pull-out tests, *Geosynthetics International*, 4 (1997) 5, pp. 509-521.
- [82] Marques, J.M.M.C.: Finite element modelling of the pull-out test of geosynthetics, *VIII International Conference on Computational Plasticity, Barcelona*, 2005.
- [83] Palmeira, E.M.: Bearing force mobilisation in pull-out tests on geogrids, *Geotextiles and geomembranes*, 22 (2004), pp. 481-509.
- [84] Palmeira, E.M.: *Soil-geosynthetic interaction: Modelling and analysis*, *Geotextiles and geomembranes*, 27 (2009), pp. 368–390.

- [85] Yu, Y., Bathurst, R.J.: Influence of Selection of Soil and Interface Properties on Numerical Results of Two Soil–Geosynthetic Interaction Problems, *International Journal of Geomechanics*, (2006), 04016136.
- [86] Shuwang, Y., Shouzhong, F., Barr, B.: Finite-element modelling of soil-geogrid interaction dealing with the pullout behaviour of geogrids, *Acta Mechanica Sinica*, 14 (1998) 4, pp. 371–382.
- [87] Teerawattanasuk, C., Bergado, D.T., Kongkitkul, W.: Analytical and numerical modeling of pullout capacity and interaction between hexagonal wire mesh and silty sand backfill under an in-soil pullout test, *Canadian Geotechnical Journal*, 40 (2003), pp. 886 – 899.
- [88] Palmeira, E., Dias, A.C.: Numerical Analysis of Soil–Reinforcement Interaction, The First Pan American Geosynthetics Conference and Exhibition, Cancun, Mexico, 2008.
- [89] Rouse, P., Fannin, R.J., Taiebat, M.: Sand strength for back-analysis of pull-out tests at large displacement, *Géotechnique*, 64 (2014), pp. 320.
- [90] Mosallanezhad, M., Taghavi, S.H., Hataf, N., Alfaro, M.C.: Experimental and numerical studies if the performance of the new reinforcement system under pull-out conditions, *Geotextiles and Geomembranes*, 44 (2016), pp. 70–80.
- [91] Dafalias, Y.F., Hermann, L.R.: Bounding surface plasticity. II: Application to isotropic cohesive soils, *Journal of Engineering Mechanics ASCE*, 112 (1986) 12, pp. 1263–1291.
- [92] Bjerrum, L., Kringstad, S., Kummeneje, O.: The shear strength of a fine sand, 1961.
- [93] Skejić, A.: Numeričko modeliranje utjecaja interakcije armature i nekoherentnog zasipa u proračunu stabilnosti zidova od armiranog tla, *Disertacija, Građevinski fakultet Sveučilišta u Zagrebu*, 2017., pp. 374.
- [94] Brinkgreve, R.B.J.: PLAXIS – Finite Element Code for Soil and Rock Analyses: Users Manual – Version 8, A.A. Balkema, Rotterdam, Netherlands, 2002.
- [95] Itasca, F.L.A.C.: Fast Lagrangian Analysis of Continua, Version 4.0 User's Guide, Itasca Consulting Group. Inc., Thrasher Square East, pp. 708, 2002.
- [96] Hussein, M.G., Meguid, M.A.: Three-dimensional finite element analysis of soil-geogrid interaction under pull-out loading condition, *GeoMontreal, 66<sup>th</sup> Canadian Geotechnical Conference, Canadian Geotechnical Society, Montreal, Quebec, Canada*, pp. 452–458, 2013.
- [97] ABAQUS: ABAQUS User's Manuals, Version 6.13., Dassault Systems Simulia Corp., Providence, RI, USA, 2013.
- [98] Wang, Z., Jacobs, F., Ziegler, M.: Visualization of load transfer behaviour between geogrid and sand using PFC 2D., *Geotextiles and Geomembranes*, 42 (2014) 2, pp. 83–90.
- [99] Tran, V.D.H., Meguid, M.A., Chouinard, L.E.: A finite–discrete element framework for the 3D modeling of geogrid–soil interaction under pullout loading conditions, *Geotextiles and Geomembranes*, 37 (2013), pp. 1–9.
- [100] Chen, C., McDowell, G.R., Thom, N.H.: Investigating geogrid-reinforced ballast: Experimental pull-out tests and discrete element modelling, *Soils and Foundations*, 54 (2014) 1, pp. 1–11.
- [101] Bathurst, R.J., Ezzein, F.M.: Geogrid pull out load–strain behaviour and modelling using a transparent granular soil, *Geosynthetics International*, (2016), pp. 1–16.
- [102] McDowell, G.R., Haireche, O., Konietzky, H., Brown, S.F., Thom, N.H.: Discrete element modelling of geogrid-reinforced aggregates, *Proceedings of the Institution of Civil Engineers-Geotechnical Engineering*, 159 (2006) 1, pp. 35–48.
- [103] Wang, Z., Jacobs, F., Ziegler, M.: Experimental and DEM investigation of geogrid–soil interaction under pullout loads, *Geotextiles and Geomembranes*, 44 (2016) 3, pp. 230–246.
- [104] Miao, C.X., Zheng, J.J., Zhang, R.J., Cui, L.: DEM modelling of pull out behaviour of geogrid reinforced ballast: The effect of particle shape, *Computers and Geotechnics*, 81 (2017), pp. 249–261.
- [105] Chen, W.B., Zhou, W.H., Jing, X.Y.: Modelling Geogrid Pull out Behaviour in Sand Using Discrete-Element Method and Effect of Tensile Stiffness, *International Journal of Geomechanics*, 19 (2019) 5, 04019039 (1–13).
- [106] Jaky, J.: The coefficient of earth pressure at rest, *Journal of the Hungarian Society of Architects and Engineers*, 25 (1944), pp. 355–358.